

The Effect of Wing Setae on Rotational Lift in Mosquito Flight

Patrick Shorey for Dr. Rival | November 29, 2019

1 Summary

Mosquito flight is notable for employing a high-frequency, short-flap wing stroke. The geometry of the wing stroke means that the wing spends a greater proportion of the stroke cycle in rotational motion, compared to other hovering insects. This suggests a greater reliance on lift due to rotation and pitching than translation and plunging. Mosquito wings are also notable for the size and abundance of setae on the dorsal surface and trailing edge. The effect of the setae on rotational lift is investigated by modelling mosquito wings as rotating ellipses, based on a quasi-steady, 2-dimensional, inviscid model. This model did not predict a significant increase in lift, when applied to the measured kinematics of a sample mosquito.

2 Mosquito Hovering Flight Kinematics

Among the insects, mosquito flight is notable for employing high aspect ratio wings, flapping at high frequency, and having short flapping strokes [1]. It is the high frequency flapping that produces the characteristic whine [2], with wing beat frequencies in males around 750 Hz [1] [3]. In Figure 1 the Reynolds number Re (1) and reduced frequency k (2) of mosquito hovering flight is compared to the hovering flight of fruitflies [1], honeybees [4], hawkmoths [5], thrips [6] and dragonflies [7]. In hovering flight, the characteristic speed U_∞ is defined as the wing tip speed, where f is wing beat frequency, Φ stroke amplitude, and R wing length. The characteristic length is the mean chord c_m , and ν the kinematic viscosity. Note, k then reduces to a measure of the aspect ratio and stroke length, with short stroke lengths and low aspect ratios being more unsteady. The definition in (2) is not universal in the literature, but common enough.

The Strouhal number similarly reduces to a relationship between the stroke height θ and stroke length ϕ (3). The flight parameters in this study, given in Table 1, give a Strouhal number of 0.08. This is low compared to typical cruising flight numbers of $0.2 < St < 0.4$ [8]. This suggests that plunging is a less significant mechanism for lift generation in mosquitoes.

$$Re = \frac{U_\infty c_m}{\nu} = \frac{2\Phi f R c_m}{\nu} \quad (1)$$

$$k = \frac{\pi f c_m}{U_\infty} = \frac{\pi c_m}{2\Phi R} \quad (2)$$

$$St = \frac{f\theta R}{U_\infty} = \frac{\theta}{2\Phi} \quad (3)$$

The above analysis suggests that mosquitoes have an unsteady wing stroke, where a greater proportion of the stroke cycle is spent in rotational motion than other insects. The rotation is known as the pronation and supination, when the wing pitches through the vertical to maintain a positive relative angle of attack. Accordingly, mosquitoes should have a diminished reliance on the translation and plunging portion of the wing stroke than other insects.

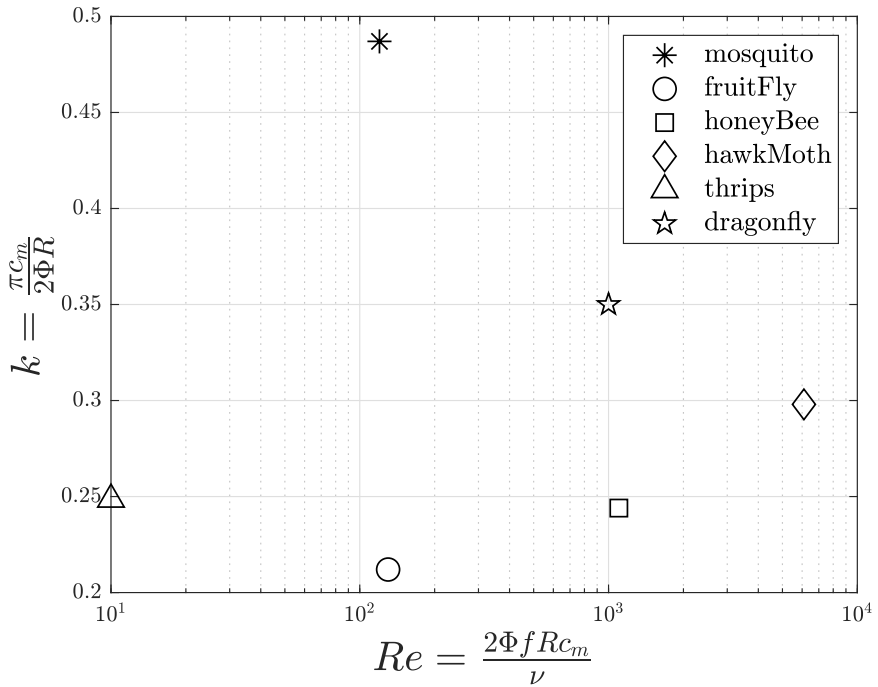


Figure 1: Comparison of mosquito flight to other hovering insects. In hovering flight k becomes a measure of the wing aspect ratio and stroke length. The short stroke length of the mosquito gives it a significantly higher reduced frequency compared to other hovering insects.

3 The Wing Fringe and Dorsal Setae

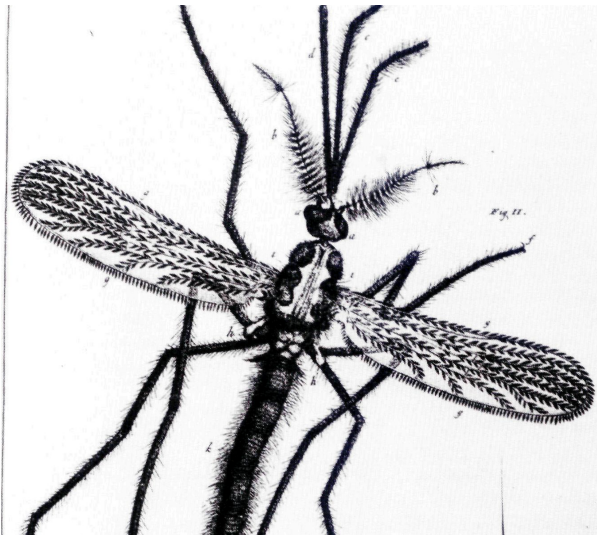


Figure 2: Illustration by Jan Swammerdam showing prominent setae features on the wings of a mosquito, shown here as petals or leaves. 17th century [9].

A conspicuous feature of the mosquito wing is the setae, hair or petal-like structures that grow out of veins on the dorsal surface, and cover the trailing edge in the characteristic *wing fringe*. A close-up of the wing fringe is shown in false colour in Figure 3. In early anatomical illustrations the setae dominate the sketch, as seen in Figure 2 [9]. This is in contrast to the most recent characterizations of mosquito flight, where the wing fringe receives summary treatment, either assumed to behave as an extension of the wing surface, shown in Figure 4 [1], or ignored altogether, as shown in Figure 5 [10]. The dorsal setae are well documented, as their colouring aids in species identification, but are ignored in the context of

aerodynamics.

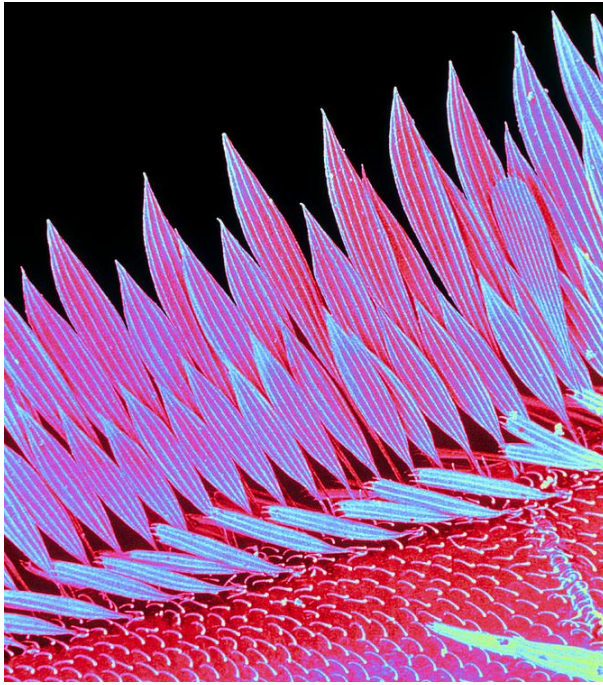


Figure 3: Mosquito wing fringe, source: fineartamerica.com

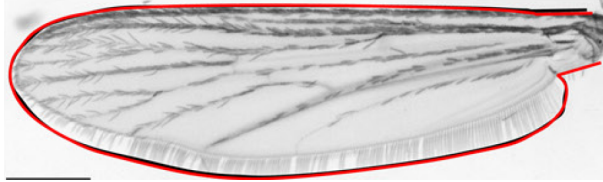


Figure 4: Wing fringe approximated as an increase in wing area, from [1].



Figure 5: Mosquito wing approximation with wing fringe omitted, from [10].

Wing setae are not unique to mosquitoes, but appear out of proportion for a wing operating at $Re \approx 10^2$. This can be seen when comparing the mosquito to its nearest neighbour by Re , the fruit fly, for which a wing is shown in Figure 6. The setae can be seen, but are much smaller. A fruit fly wing is of similar length to a mosquito's [11]. I believe part of the reason the setae are ignored is because they are common among the smallest flying insects, such as thrips and fairyflies, see Figure 7. In the smallest of these the wing becomes almost entirely made up of bristles (up to 95% in Ptiliidae Primorskiella [12]). Analytical, numerical and physical experiments with comb-like plates, inspired by thrips and fairyfly wings, have shown that a 'feather-wing' can have similar aerodynamic performance to a flat plate at $Re \leq 10$; though at $Re = 10^2$ the 'leakiness' increases significantly [13]. The benefit of the feather-wing is usually hypothesized as weight reduction, with additional arguments that it may be advantageous for clap-and-fling flight [14].

The applicability of these studies to mosquito flight is not without peril; the feather-wings are made up of setae with circular cross-sections, usually modeled as cylinders. This is in contrast to the mosquito,

where the fringe is made of overlapping scales. Additionally, most analyses are based on steady-state behaviour. If the wing fringe only offered cheap wing area, we would expect to see similar sized structures for wings at the same Re , which we don't. Additionally, this hypothesis does not explain the setae on the dorsal surface. Since mosquito wing kinematics are dominated by rotation, perhaps the setae serve a particular function producing rotational lift.

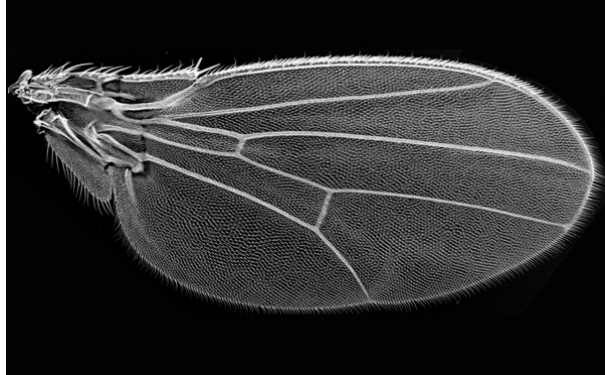


Figure 6: Fruitfly wing, source: cerebrovortex.com

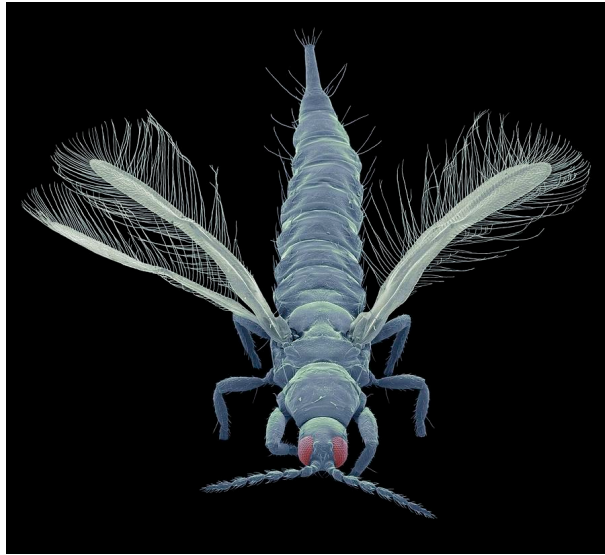


Figure 7: Thrips, source: pixels.com

4 Modelling Rotational Lift

In order to investigate the effect of setae on rotational lift, an analytical model of the rotational component of lift is required. The simplest is a quasi-steady, 2D, inviscid model based on pitching of an aerofoil (4), as presented by Taha et al. [15] and Sane and Dickinson [16]. In this expression $\dot{\eta}$ is the pitching angular velocity $\dot{\alpha} = \omega$ and \hat{x}_0 is the chord-normalized position of the pitch axis from the leading edge.

$$L(r, t)_{rot} = \rho U \left[\pi c^2 \dot{\eta} \left(\frac{3}{4} - \hat{x}_0 \right) \right] \quad (4)$$

$$\Gamma_{rot} = \left[\pi c^2 \dot{\eta} \left(\frac{3}{4} - \hat{x}_0 \right) \right] \quad (5)$$

$$L_{cylinder} = -\rho U_\infty (2\pi K) \quad (6)$$

This can be compared to the potential flow solution for a rotating cylinder (6), where $K = v_\theta r = \omega r^2$ is the free vortex constant evaluated at the surface, applying the no-slip condition. When $\hat{x}_0 = 0.5$ and $D = c$, $L_{rot} = \frac{1}{2}L_{cylinder}$. For insects it is thought that $0.25 < \hat{x}_0 < 0.5$ [16]. Bomphrey et al [1] observed a shifting axis of rotation throughout pronation/supination in mosquito flight, though locations weren't reported. For this analysis \hat{x}_0 has been kept constant at 0.5.

Without access to the derivation of (4) we can see that it is the same physics as (6) but with some geometric scaling. In this analysis I work with the integral expression of (6) given in (9). This allows for numeric integration over an arbitrary ellipse specified by (r, θ) co-ordinates. A comparison of the predicted sectional lift produced by a rotating ellipse versus a circle is given in Figures 8 and 9.

$$\frac{L}{b} = - \int_0^{2\pi} (p_s - p_\infty) \sin \theta r d\theta \quad (7)$$

$$= -\frac{1}{2} \rho U_\infty^2 \int_0^{2\pi} \left(\frac{4K}{U_\infty r} \sin \theta \right) \sin(\theta) r d\theta \quad (8)$$

$$= -2\rho U_\infty \omega \int_0^{2\pi} (r^2 \sin^2 \theta) d\theta \quad (9)$$

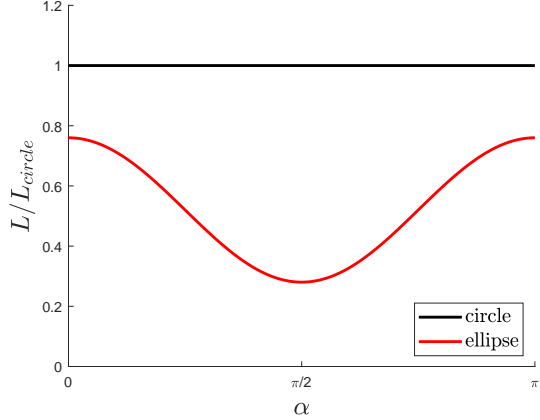


Figure 8: Instantaneous lift produced by a rotating ellipse compared to a circle of the same maximum width, as modelled by (9). For an ellipse of height/width = $\frac{1}{5}$, the lift is approximately half that of the circle, over a full rotation.

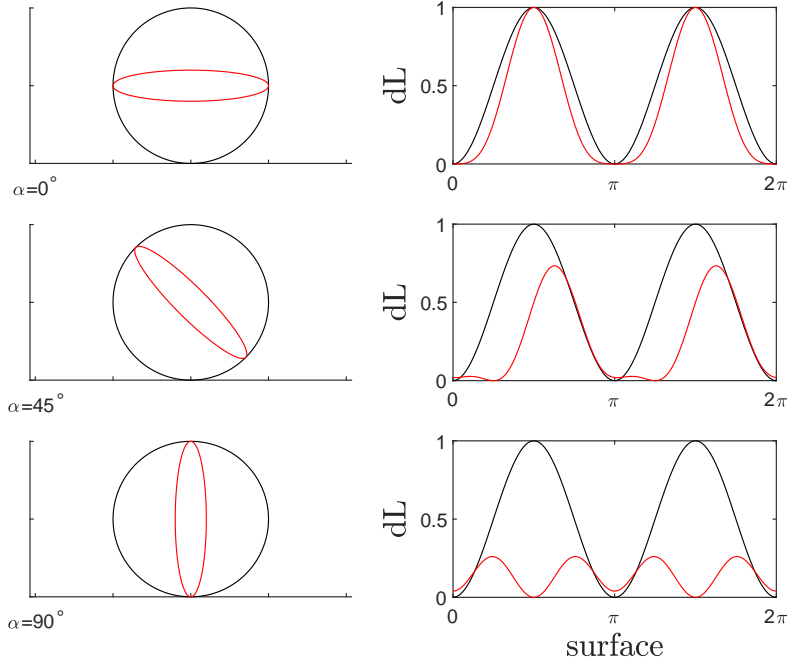


Figure 9: Instantaneous distribution of lift over the surface of a rotating ellipse, showing the effect of angle of attack. Black represents a circle of the same maximum width, red is an ellipse with height/width = $\frac{1}{5}$.

5 Modelling the Setae

From photographs such as in Figures 4 and 5, the length of the setae were approximated as $\frac{1}{10}$ of the mid-chord length c_m . It is hypothesized that the setae lift during rotation and extend the effective no-slip condition at the wing wall, giving a greater surface area over which to turn the flow. To model this effect, the lift produced by a rotating thin plate is compared to a rotating ellipse with length equal to c_m and height equal to twice the setae length ($\frac{1}{10}c_m$). Kinematics of the wing stroke are presented in Figure 10. Other parameters are listed in Table 1. The calculated lift over the stroke is shown in Figure 11. Sectional lift was found at the tip and treated as constant over the wing. This overestimated the total magnitudes, and so the relative differences are more meaningful. The total magnitudes are on the same order as calculated in the literature [1]. The total rotational lift per stroke is summarized in Table 2. Using this model, it was predicted that the presence of setae would increase rotational lift by 1.3%, compared to a thin plate.

Table 1: Mosquito parameters

R	$2.75 \times 10^{-3} m$
Φ	$0.76 rad$
c_m	$0.655 \times 10^{-3} m$
f	$750 Hz$
ν_{air}	$1.52 \times 10^{-5} m^2/s$

Table 2: Total lift per stroke, normalized by potential lift on a rotating cylinder of equal diameter.

	$L/L_{cyl.}$
ellipse	0.76
thin plate	0.75
aerofoil	0.50

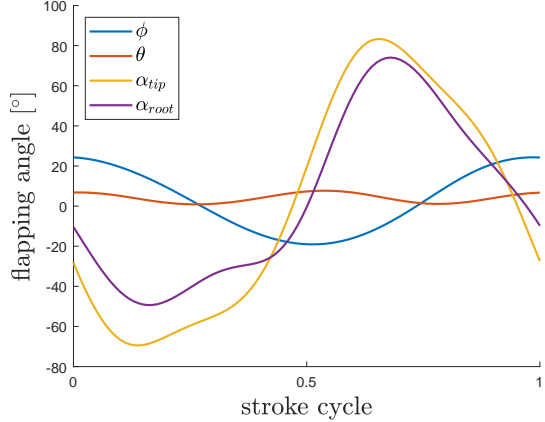


Figure 10: Measured kinematics of a sample mosquito, data from Bomphrey et al. [1]. ϕ is the in-plane stroke distance, θ is the elevation, and α is the pitch angle measured from the vertical.

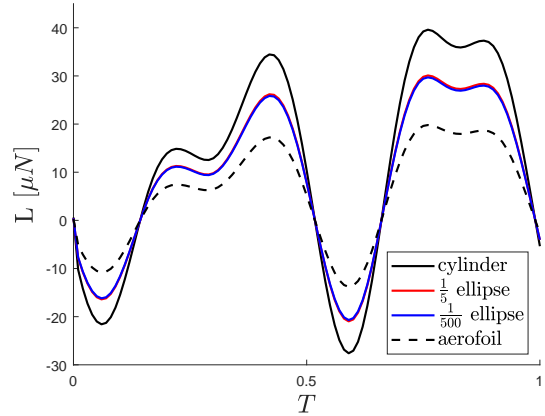


Figure 11: Rotational lift predicted by quasi-steady, 2D, inviscid models. At high aspect ratios, the predicted lift for rotating ellipses is insensitive to aspect ratio. The kinematics of the rotation are ϕ and α_{tip} from Figure 10.

6 Discussion

The rotating ellipse model is insensitive to changes in aspect ratio for high-aspect ratio ellipses, with a 100 times increase in aspect ratio leading to a 1.3% increase in predicted lift. This suggests that if the setae do aid in rotational lift the mechanism is more sophisticated than the Magnus effect. Some of the more problematic assumptions in the model are the quasi-steady and 2D assumptions. Insect flight is generally modelled as consisting of several unsteady mechanisms such as wing-wake interaction, clap-and-fling, delayed stall and added-mass effects [17]. None of these effects would be captured by a quasi-steady model. As a 2-D model it also ignores span-wise flows and effects such as tip-vortices. Certain authors have taken specific issue with the rotational circulation analogy, such as Walker [18].

It should be noted that the flapping frequencies of up to 800 Hz quoted in the literature are specific to male mosquitoes, with females at about half the speed. Mosquitoes are capable of rapid frequency changes and there is evidence they use acoustic modulation to find mates [3]. That their flight is seemingly insensitive to a wide range of flapping frequencies is another curiosity.

A final speculation is that the setae do not aid in the wing aerodynamics directly, but are feedback mechanisms for the mosquito's flight control system, capable of sensing small pressure or velocity variations in the flow over the wing. This would be analogous to the hypothesized role of feather vibration as stall warning in birds [19].

References

- [1] Richard J Bomphrey, Toshiyuki Nakata, Nathan Phillips, et al. “Smart wing rotation and trailing-edge vortices enable high frequency mosquito flight”. In: *Nature* 544.7648 (2017), p. 92.
- [2] Laura A Miller. “Biomechanics: The aerodynamics buzz from mosquitoes”. In: *Nature* 544.7648 (2017), p. 40.
- [3] Patrício MV Simões, Robert A Ingham, Gabriella Gibson, et al. “A role for acoustic distortion in novel rapid frequency modulation behaviour in free-flying male mosquitoes”. In: *Journal of Experimental Biology* 219.13 (2016), pp. 2039–2047.
- [4] Douglas L Altshuler, William B Dickson, Jason T Vance, et al. “Short-amplitude high-frequency wing strokes determine the aerodynamics of honeybee flight”. In: *Proceedings of the National Academy of Sciences* 102.50 (2005), pp. 18213–18218.
- [5] Toshiyuki Nakata and Hao Liu. “Aerodynamic performance of a hovering hawkmoth with flexible wings: a computational approach”. In: *Proceedings of the Royal Society B: Biological Sciences* 279.1729 (2011), pp. 722–731.
- [6] H Liu and Hikaru Aono. “Size effects on insect hovering aerodynamics: an integrated computational study”. In: *Bioinspiration & Biomimetics* 4.1 (2009), p. 015002.
- [7] Kakkattukuzhy M Isaac, Anthony Colozza, and Jessica Rolwes. “Force measurements on a flapping and pitching wing at low Reynolds numbers”. In: *44th AIAA Aerospace Sciences Meeting and Exhibit*. 2006, p. 450.
- [8] Graham K Taylor, Robert L Nudds, and Adrian LR Thomas. “Flying and swimming animals cruise at a Strouhal number tuned for high power efficiency”. In: *Nature* 425.6959 (2003), p. 707.
- [9] Jan Swammerdam. *The Book of Nature; or, The History of Insects*. London: Printed for CG Seyffert, 1758.
- [10] Longgui Liu and Mao Sun. “Dynamic flight stability of hovering mosquitoes”. In: *Journal of theoretical biology* 464 (2019), pp. 149–158.
- [11] Xin Cheng and Mao Sun. “Wing-kinematics measurement and aerodynamics in a small insect in hovering flight”. In: *Scientific reports* 6 (2016), p. 25706.
- [12] Alexey A Polilov, Natalia I Reshetnikova, Pyotr N Petrov, et al. “Wing morphology in featherwing beetles (Coleoptera: Ptiliidae): Features associated with miniaturization and functional scaling analysis”. In: *Arthropod structure & development* 48 (2019), pp. 56–70.
- [13] G. Davidi and D. Weihs. “Flow Around a Comb Wing in Low-Reynolds-Number Flow”. In: *AIAA Journal* 50.1 (2012), pp. 249–253. doi: 10.2514/1.j051383. URL: <https://doi.org/10.2514%2F1.j051383>.
- [14] Shannon K. Jones, Young J. J. Yun, Tyson L. Hedrick, et al. “Bristles reduce the force required to ‘fling’ wings apart in the smallest insects”. In: *The Journal of Experimental Biology* 219.23 (2016), pp. 3759–3772. doi: 10.1242/jeb.143362. URL: <https://doi.org/10.1242%2Fjeb.143362>.
- [15] Haithem E Taha, Muhammad R Hajj, and Ali H Nayfeh. “Longitudinal flight dynamics of hovering MAVs/insects”. In: *Journal of Guidance, Control, and Dynamics* 37.3 (2014), pp. 970–979.
- [16] Sanjay P Sane and Michael H Dickinson. “The aerodynamic effects of wing rotation and a revised quasi-steady model of flapping flight”. In: *Journal of experimental biology* 205.8 (2002), pp. 1087–1096.
- [17] Diana D Chin and David Lentink. “Flapping wing aerodynamics: from insects to vertebrates”. In: *Journal of Experimental Biology* 219.7 (2016), pp. 920–932.
- [18] Jeffrey A Walker. “Rotational lift: something different or more of the same?” In: *Journal of Experimental Biology* 205.24 (2002), pp. 3783–3792.
- [19] Christoph Brücker, Daniel Schlegel, and Michael Triep. “Feather vibration as a stimulus for sensing incipient separation in falcon diving flight”. In: *Natural Resources* 7.07 (2016), pp. 411–422.